2015-06-01

Friction Bit Joining of Dissimilar Combinations of DP 980 Steel and AA 7075

Rebecca Hilary Peterson
Brigham Young University

Friction Bit Joining of Dissimilar Combinations of DP 980 Steel and AA 7075

Rebecca Hilary Mercy Peterson

A thesis submitted to the faculty of
Brigham Young University
in partial fulfillment of the requirements for the degree of

Master of Science

Michael P. Miles, Chair
Andrew R. George
Steven L. Shumway

School of Technology

Brigham Young University

June 2015

ABSTRACT

Friction Bit Joining of Dissimilar Combinations
of DP 980 Steel and AA 7075

Rebecca Hilary Mercy Peterson
School of Technology, BYU
Master of Science

Friction Bit Joining (FBJ) is a new technology that allows lightweight metals to be joined to advanced high-strength steels (AHSS). Joining of dissimilar metals is especially beneficial to the automotive industry because of the desire to use materials such as aluminum and AHSS in order to reduce weight and increase fuel efficiency.

In this study, FBJ was used to join 7075 aluminum and DP980 ultra-high-strength steel. FBJ is a two-stage process using a consumable bit. In the first stage, the bit cuts through the top material (aluminum), and in the second stage the bit is friction welded to the base material (steel). The purpose of the research was to examine the impact a solid head bit design would have on joint strength, manufacturability, and ease of automation. The solid head design was driven externally. This design was compared to a previous internally driven head design. Joint strength was assessed according to an automotive standard established by Honda.

Joints were mechanically tested in lap-shear tension, cross-tension, and peel configurations. Joints were also fatigue tested, cycling between loads of 100 N and 750 N. The failure modes that joints could experience during testing include: head, nugget, material, or interfacial failure. All tested specimens in this research experienced interfacial failure. Welds were also created and examined under a microscope in order to validate a simulation model of the FBJ process. The simulation model predicted a similar weld shape and bond length with 5 percent accuracy.

Joints made with external bits demonstrated comparable joint strength to internal bits in lap-shear tension and cross-tension testing. Only external bits were tested after lap-shear tension, because it was determined that external bits would perform comparably to internal bits. Joints made with external bits also exceeded the standard for failure during fatigue testing. Peel tested specimens did not meet the required strength for the automotive standard. Examining specimens under a microscope revealed micro-cracks in the weld. These defects have been shown to decrease joint strength. Joint strength, especially during peel testing, could be increased by reducing the presence of micro-cracks. The external bit design is an improvement from the internal bits for manufacturability and ability to be automated, because of the less-expensive processes used to form the bit heads and the design that lends to ease of alignment.

Keywords: Rebecca Peterson, friction bit joining, FBJ, dissimilar metals, advanced high-strength steel, aluminum, DP980, automotive manufacturing, joint strength

ACKNOWLEDGEMENTS

I wish to thank Dr. Mike Miles for his support and guidance. I would also like to thank my committee members and other professors in the manufacturing program at Brigham Young University. Thank you to Ruth Ann Lowe for her impressive organization skills and kindness.

I feel great appreciation for the great team of undergraduates I had to work with: Alex Avila, Kevin Shirley, and Aislinn Macintosh. Their willingness and teamwork made this journey an enjoyable experience.

Thank you to my parents and siblings for raising me to achieve my goals. Thank you, especially, to Elyssa for her punctuation expertise. Most importantly, my sincerest love and appreciation is to my husband, Cody. Thank you for supporting me and never letting me get discouraged. Thank you for reminding me that things always work out.

TABLE OF CONTENTS

LIST OF TABLES

LIST OF FIGURES

1 INTRODUCTION

Government regulations on fuel efficiency in the automotive industry have become more restrictive in recent years (The Federal Reserve, 2012). In order to meet the enforced regulations, many auto companies have implemented design changes to make their products lighter (Caffrey, 2013). One method that is gaining momentum is the use of aluminum in the body structure where steel has been used in the past. Design changes also include the use of advanced high-strength steel (AHSS), which allows for downgauging, or the use of thinner gauge metal. The combining of aluminum and AHSS have created a challenge in manufacturing because of difficulties in using resistance spot welding or self-piercing riveting to join them together.

AHSS and light metals, like aluminum, cannot be joined with typical welding processes. The considerable difference in melting temperatures, ductility, and hardness contribute to the need for alternative joining processes (Mishra, 2014). The high alloy content of AHSS contributes to the challenges of joining AHSS with traditional welding processes, and the challenges are magnified when trying to join AHSS to lightweight materials.

The pressing need in industry has led to the development of several technologies that attempt to overcome the challenge of joining AHSS and aluminum. Methods such as friction stir welding, resistance spot welding with an intermediate layer of material, and friction stir spot welding employ friction to join the dissimilar metals. Friction stir spot welding is the closest to achieving the required bonding for the automotive industry (Feng, 2005). Other technologies,

such as adhesives and self-pierce riveting, are applicable to some alloy combinations, but are less successful when the higher strength AHSS are used (Abe, 2009). Although these methods overcome some of the difficulties associated with joining AHSS and light metals, they are not successful when higher-strength AHSS is combined with aluminum.

Friction bit joining (FBJ) is a new technology that overcomes some of the limitations and challenges of other joining techniques. The flexibility, short cycle times, and quality of joints, that have been demonstrated in prior work show that FBJ is a feasible alternative to traditional methods for joining of aluminum and steel for body applications (Weickum, 2011). FBJ is a two-stage process performed on a machine specifically designed for the required process conditions. The first stage is the cutting stage, where the consumable bit cuts through the lighter top material. In the second stage, the bit is friction welded to the lower material, forming a primary bond. The bit material and lower metal material are similar alloys that are compatible for creating a strong, metallurgical bond. The bit remains in the newly created joint.

Though relatively new, FBJ has proven to have greater joint strength to these other methods while having more flexibility in joining very hard materials to softer materials (Squires, 2014). Research on FBJ includes areas such as feasibility, optimal parameters, and bit alloy and design. Although different aspects of the bit design have been explored, the head design and method of driving the bit, whether internal or external, has not been optimized.

1.1 **Purpose of the Research**

The purpose of this research is to evaluate a bit design for friction bit joining according to performance criteria set by one of the sponsors. The bit will be externally engaged, and joints

made with the bit will be tested in three configurations and fatigue. Manufacturability and ease of automation will be considered for the new bit design.

1.2 **Research Hypotheses**

- A solid bit design will yield comparable joint strength to a hollow design. This joint strength will meet the criteria established for automotive standards. The required joint strengths are greater than 5 kN for lap-shear tension, 1.5 kN for cross-tension, 1.5 kN for peel, and greater than ten million cycles for fatigue testing.

1.3 **Objectives**

- The objective of this research is to demonstrate success in coupon scale joining of advanced high strength steel (AHSS) to high strength aluminum (HSA) by friction bit joining (FBJ) using externally driven bits.
- A model will also be developed in order to study the process. Welding temperatures and bond area will be predicted by the model and compared with experimental data.

2 LITERATURE REVIEW

Lightweight construction will impact the automotive industry through the development of new technologies, new materials, new products, and environmental affects (Albrecht, 2013). High-strength materials with good combinations of strength, formability, fatigue resistance, and toughness are required by current automotive designs. Auto makers have recognized that using different materials in the auto body can optimize design performance. A variety of different higher-strength materials are incorporated into assemblies. One common material being employed is AHSS (Matlock, 2009).

Increased requirements for fuel economy, crash safety, and vehicle performance has resulted in competitive development within the steel and light-weight metal industries. The steel industry's answer to the requirements is the introduction of AHSS. These steels can be characterized as having reasonable formability and ductility properties while maintaining high strength (Kuziak, 2008).

First generation AHSS are grouped into the categories of dual phase (DP), transformation induced plasticity (TRIP), complex phase (CP), and martensitic steels (MART) (Matlock, 2009). The use of these AHSS allows automotive companies to use thinner-gauge sheets in the body structure. AHSS also have higher energy absorption for dynamic loading, making them ideal for crash worthiness and improved passenger safety. AHSS are much less formable than mild steels,

but are more formable than typical HSS. The ability to form HSS decreases as strength increases. However, AHSS combines high strength and formability.

Using a variety of materials, including AHSS and aluminum, creates challenges in joining (Mishra, 2014). The challenge of joining dissimilar metals is the varying melting temperatures, ductilities, and hardnesses. Especially challenging is joining AHSS and light metals. AHSS has higher contents of alloying elements than lower-strength steels. This makes AHSS more sensitive to the welding thermal cycle, resulting in greater variations of microstructures and properties of welds. There are a variety of technologies that attempt to overcome these challenges.

Resistance spot welding (RSW) is a common welding method in the automotive industry used for joining steel sheets. Its high operating speeds and ease of automating make RSW a critical technique for joining in automotive applications. In RSW, heat is generated by "the resistance of the parts being welded by the flow of a localized electrical current" (Pouranvari, 2013). To ensure adequate contact, pressure is applied to the parts being welded. AHSS experiences complicated microstructure transformations during RSW, specifically the designed microstructure is destroyed in the fusion zone (FZ) and the heat affected zone (HAZ) (Pouranvari, 2013). RSW has been proven to join AHSS to softer metals, but micro-cracks form in the joint, creating weak points (Miles, 2010). A tactic to facilitate the joining of aluminum and steel is to introduce a cold-rolled clad material as an intermediate layer (Sun, 2004). However, this additional material would increase material costs as well as vehicle weight. These weaknesses limit the use of RSW for automotive applications of joining AHSS with lighter-weight materials.

Friction stir welding (FSW) was developed in 1991. The advantages of FSW are a minimum HAZ, short cycle times, and good quality welds. Temperatures that are developed through friction are less than the melting point of the workpiece metal (Rhodes, 1997). Friction stir spot welding (FSSW) is a commonly used method for joining aluminum and steel sheet metal in the automotive industry. However, its applications are limited, because friction stir spots welds of aluminum and steel have been shown to have relatively low joint strength. For welding steel, FSSW can reduce the thermal effect to the welded material, because it is a solid-state process. However, the high-speed, high-volume, and cost-conscious nature of the automotive industry restricts the implementation of FSSW, because tooling cost is quite high compared to RSW (Feng, 2005).

Another technology for joining dissimilar metals is self-piercing riveting (SPR). SPR drives the shank of the rivet though the upper sheet metal and flares the skirt of the rivet in the lower sheet. This creates an interlock. SPR is a cold-joining process. It is also a relatively fast process and is low energy. SPR has proven to join aluminum and steel and is used in today's production. A limitation of this process is that piercing the rivet into the AHSS is difficult, because the strength of the steel sheets approaches that of the rivet. Steels with ultimate tensile strengths below 590 MPa can be joined with aluminum alloys (Abe, 2009). However, the higher strength steels are not ductile enough to form around the rivets of SPR. Increasing the strength of the rivet is also limited (Mori, 2014). The size of the riveting gun also restricts access to certain joint areas. Due to the crevices and surface irregularities, corrosion is also a concern (Barnes, 2000).

Adhesives are another common technique for joining dissimilar metals. A few advantages of adhesives are that they do not distort the components being joined, a continuous bond is

produced rather than a localized point contact, the equipment is lower in cost, and the bonds are inherently high strength in shear. Disadvantages include that the adhesives are generally epoxy or solvent-based, which brings more environmental concerns, many structural adhesives require heat curing, and the joints created are weak in peel. This peel limitation would be especially worrisome for crashworthiness in vehicles (Barnes, 2000).

These different processes meet some of the needs for joining AHSS and aluminum. There are still gaps in their performance and processes. Friction bit joining overcomes many of these limitations while still meeting performance and manufacturing requirements.

Friction bit joining is a relatively new technology. It has been proven to have comparable joint strength to these other methods while having more flexibility in materials. Research on FBJ includes areas such as feasibility, optimal parameters, and bit alloys and design (Weickum, 2011). Materials that have been explored include cast-iron, carbon fiber, Al 5574, Al 7075, DP980, and DP590 (Miles, 2010, 2013). Research examining the microstructure of FBJ welds concluded that a defect-free joint can be successfully produced with FBJ (Huang, 2009). Additional research compared a "fluted" bit to a "flat" bit design. The flutes were intended to aid in removing chips that form during the cutting phase of joining. The "fluted" design was found to produce more consistent results (Miles, 2010). This research conducted by Miles et al. has shown that a short weld cycle time produces improved joint strength, and the material and design of the bit will affect joint strength. Recent research at Brigham Young University studied the relationship between weld strengths and the programmed parameters of Z-axis velocity, RPM, and Z-axis command (Squires, 2014). The research on programmed parameters found that a short weld cycle time yielded the best joint results. Slower RPM's shear the bit and create weaknesses in the bit. Corrosion testing has been conducted on FBJ welds with and without an

added adhesive layer. This research on adhesives found that although the added layer was effective in maintaining the mechanical integrity of the joints in the presence of a corrosive medium, it provided essentially no increase in joint strength over FBJ welds without an adhesive layer (Lim, 2015). An area of FBJ that has not been investigated yet, which my research focused on, is bit head design.

3 EXPERIMENTAL DESIGN

The questions and hypotheses of this research were explored using welds made through friction bit joining. Two head designs were compared: an externally driven design and an internally driven design. Externally driven means that the bit is gripped and engaged on the outer portion of the head. Internally driven bits contain a cavity at the center of the top of the head. These bits are engaged through this cavity, and the main force for driving is applied to the internal portion of the cavity. The concept of an externally driven bit head design had not been investigated in previous research. The integrity of the joints were tested in four different configurations, as required by automotive standards. These configurations were lap shear tension, cross-tension, peel, and fatigue. A simulation was also developed to predict material flow, bond area, and welding temperature of the FBJ process. The simulation model was validated with experiments.

3.1 FBJ Process and Phases

Specimens were made by FBJ. The FBJ process is a two-stage process using a consumable bit. The first stage is the cutting phase. A bit is inserted into the corresponding driver (external or internal), and then the bit is engaged and driven and cuts through the top lightweight material. In the second stage, the bit is friction welded to the base material. The bit and base

materials are similar, and so fusion is possible. The design of the bit heads holds the top material against the base material. This is how joints are created. Figure 3-1 shows a simplified schematic of an FBJ weld.

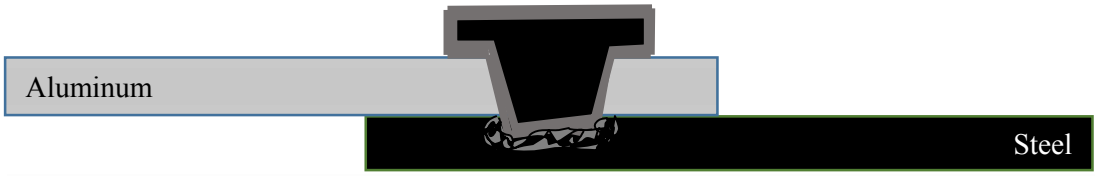

Figure 3-1: Process Schematic

3.2 **FBJ Machine**

The FBJ machine (Figure 3-2), made by MegaStir Technologies, was engineered and built specifically for this process (Squires, 2014). Servo motors provide precise control of spindle rotation, spindle speed, and movement of the spindle in the Z direction. A motor mounted on the frame controls Z-axis movement and is able to apply high loads during the weld cycle. A variety of tool holders can be mounted into the chuck placed in the end of the spindle. The FBJ process requires rapid stopping ability. Therefore, a brake device on the spindle was incorporated into the machine design. Specimens are positioned and secured on a fixture below the spindle. An additional clamp was placed on top of the specimens to ensure they were adequately positioned and secured. The force used to secure the clamp could be measured and then remain constant through all welds. Locating pins were also used to ensure proper alignment and placement.

Figure 3-2: FBJ Machine

Information and feedback on net Z force, Z motor torque, Z axis velocity, spindle RPM, spindle torque, weld duration and tool depth are provided by two sensors. The software that operates the machine records the data gathered by these sensors during each weld cycle. Machine control is also enabled by this software. Settings such as spindle RPM, Z axis velocity (in/min), Z travel command (in) and dwell time (ms) are entered into the computer interface before each weld cycle. The software also allows up to four separate stages to be activated or deactivated during the weld cycles. The specimens created for this research's experiments used only two stages. Table 3-1 shows the settings of process variables used for experiments.

Table 3-1: Processing Parameters

Parameter:	Stage 1:	Stage 2:
Spindle RPM	2,000	2,500
Z-Velocity (in/min)	8.875	8.875
Z-Command (in)	-0.077	-0.187
Dwell Time (ms)	0	0

3.3 **Bit Material, Design, and Production**

Previous research in FBJ used an internally driven bit. The shaft of the bit had cutting flutes for cutting through the aluminum and promoting chip removal. The bit head had a "torx" design in the center that the driver engaged for welding. When the welds were examined under a microscope, it was found that the sides of the bit's head were collapsing in. This created voids in the joint and, therefore, weak points. These voids can be seen in Figure 3-3. It was believed that an externally driven bit head would increase the performance of FBJ welds because of the elimination of the internal pockets**.**

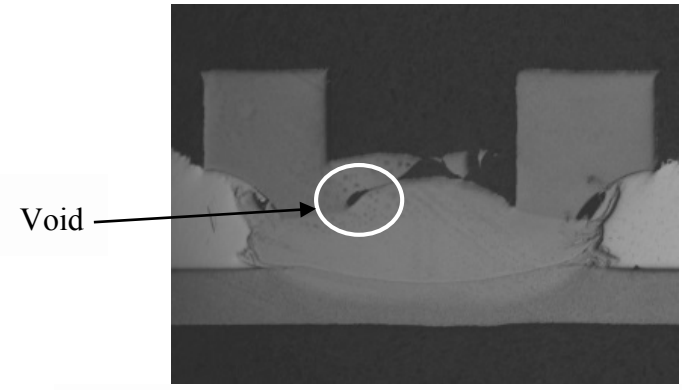

Figure 3-3: Collapsed Internal Bit Creating Weak Points

The external bits maintained the shaft design of the previous internal bits. The head was the only portion that was modified. The material used for both external and internal bits was

AISI 4140 alloy steel. This material has high fatigue strength, impact and abrasion resistance, toughness, ductility, and torsional strength. Molybdenum and chromium are the strengthening agents of the microstructure.

The first step to manufacture both bits was to create a blank (Figure 3-4) using an Okuma Space Turn LB300-M CNC lathe. The blanks contained the profile of the bits, including cutting flutes. Creating the head design into the blanks was a different process for internal and external bits. A rotary broach process was used to manufacture heads of the internal bits (Figure 3-5). The bit blanks were placed in a fixture that was then inserted into the CNC lathe. The fixture was necessary in order to provide adequate surface area for the CNC lathe chuck to grip. A rotary broach then cut a T-25 Torx pocket in the head of the blanks.

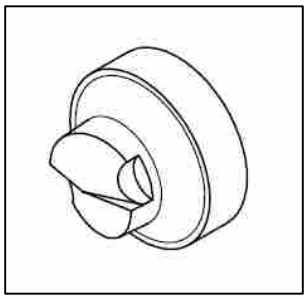

Figure 3-4: Bit Blanks

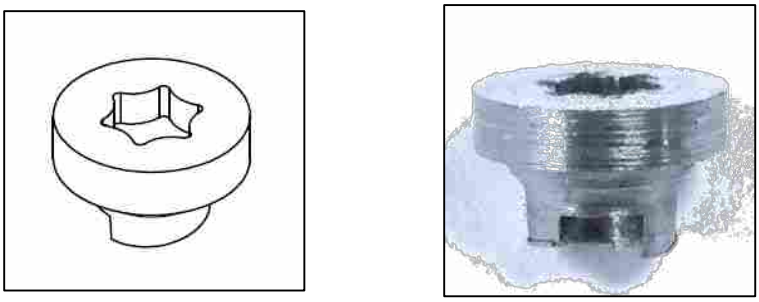

Figure 3-5: Internal Bits

The heads of the externally driven bits (Figure 3-6) were manufactured using a forming process. After the turning process for the blanks, a small diameter protrusion (pip) would remain on the head of the blank. This was ignored for the internal bit process, because the head cutting process removed this excess material. For forming external bits, however, this excess material had to be ground off before being formed with a die. The two-piece forming die was machined out of D2 steel. The top piece contained the pattern for the bit head. This pattern was created using a ram EDM. The top piece was then heat treated to reach a 60 Rockwell C hardness. The bottom piece had a center hole for the shaft of the blanks to be inserted into. Three offset holes were drilled into both pieces, with pins in the base holes for alignment. A blank bit would be placed shaft-down into the bottom piece. The top piece was placed with the aligning pins. A pneumatic press was used to force the two halves together and form the head of the bits. There was no post processing required after the heads were formed.

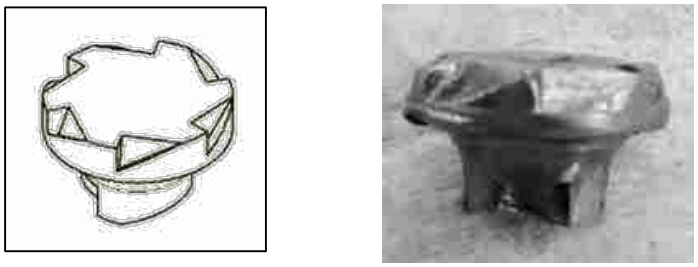

Figure 3-6: External Bits

The two different head designs required two different drivers for engaging. The internal driver (Figure 3-7) was an adaptation of a DeWalt Magnetic tool holder typically used with hand drills. The tool holder was modified to make it more compatible with the collet of the FBJ machine. A “cap” was also added to maintain pressure on the flat top of the bit head during welding.

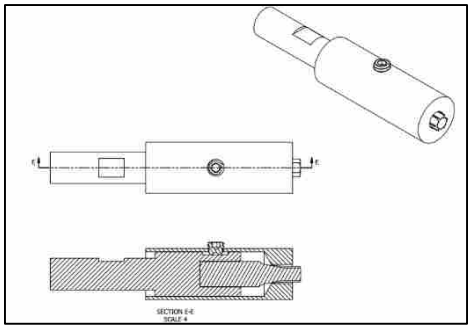

Figure 3-7: Internal Bit Driver

The driver for external bits (Figure 3-8) was machined out of ½ inch D2 steel bar stock. A ram EDM was used to create the head shape into the stock. The material was then turned on a manual lathe to have the correct diameters for the FBJ machine. A 0.40 inch hole was drilled through the center of the head shaped end for placement of a magnet. Once all machining was completed, the material was heat treated to approximately 50 Rockwell C hardness. The magnet was inserted after heat treating.

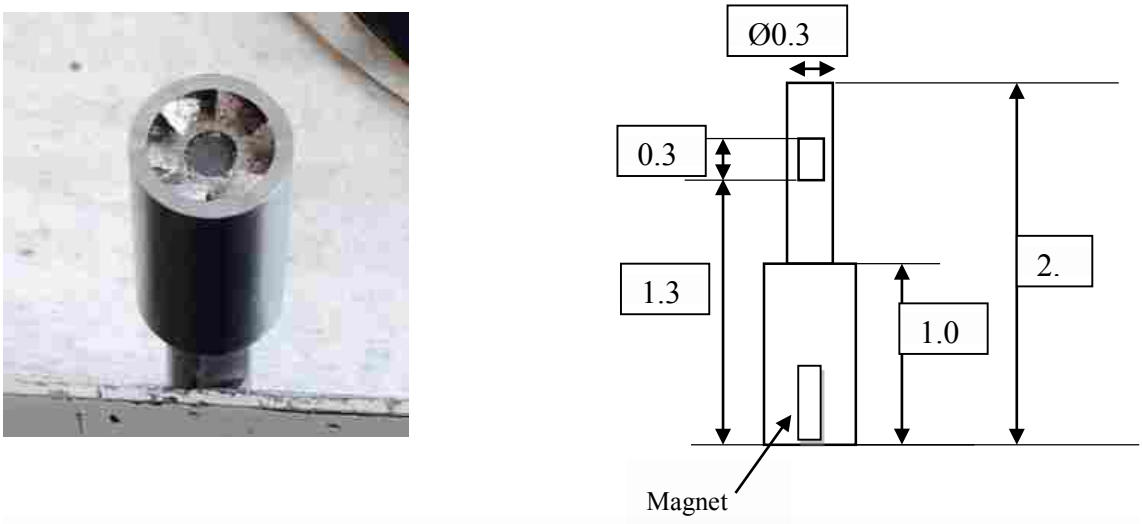

Figure 3-8: External Bit Driver

3.4 **Coupon Material**

Aluminum and steel coupons used in the experiments had 2 millimeter and 1.2 millimeter thickness respectively. The coupons were cut on a hydraulic shear with the grains running length wise.

The steel used as a base material in the experiments was the AHSS, DP980. DP980 is a dual phase steel consisting of a ferrite matrix containing hard martensitic second phase in the form of islands. The microstructure of DP980 is shown in Figure 3-9 (Lim, 2015). The presence of martensite increases the tensile strength. DP980 is expected to have a minimum ultimate tensile strength of 980 MPA. The generally continuous soft ferrite phase results in excellent ductility for its high strength. Table 3-2 shows the mechanical properties for DP980 (Taylor, 2014). The high strength, strain hardenability, and fatigue resistance make DP980 an ideal material for automotive applications.

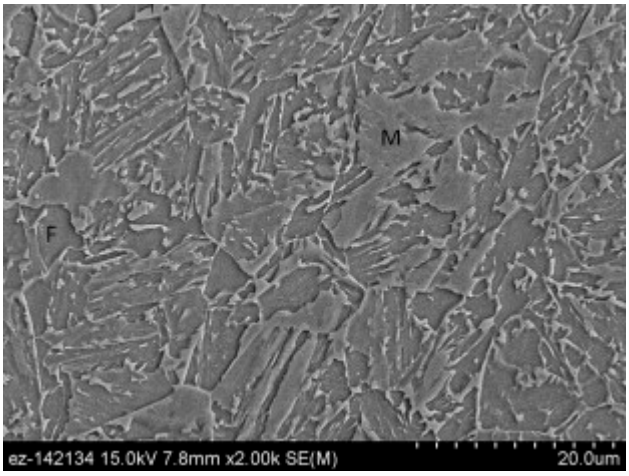

Figure 3-9: Microstructure of DP 980, Consisting of Ferrite (F) and Small Islands of Martensite (M)

Table 3-2: DP980 Mechanical Properties

Material	Thickness (mm)	Yield Strength (Mpa)	Ultimate Tensile Strength (Mpa)	Elongation (%)
DP980	1.2	727	984	12.5

Aluminum 7075-T6 was used as the light-weight material in the experiments. Zinc is the primary alloying element (Alcoa). Aluminum 7075-T6 demonstrates high strength while maintaining low density. This makes it a good candidate for transportation applications such as aerospace and automotive structures. The 7075 alloy combines high strength with moderate toughness and corrosion resistance. Table 3-3 shows the mechanical properties of AA7075 (Alcoa).

Table 3-3: AA 7075 Mechanical Properties

Material	Thickness (mm)	Yield Strength (Mpa)	Ultimate Tensile Strength (Mpa)	Elongation (%)
AA 7075-T6	0.203-6.32	434-476	510-538	5-8

3.5 **Automotive Standards for Spot Joint Performance**

Joint performance was evaluated according to criteria determined by the sponsor Honda. This criteria defines specifications ensuring that the joint will perform as needed when put into service. The standard thresholds for joint performance are given in Table 3-2. The steel baseline is given for a reference.

Table 3-4: Joint Standards for Automotive Industry

	Steel Baseline	Steel-Al Mechanical Joint
Lap Shear Tension (TSS)	>18kN	>5kN
Cross-tension (CTS)	>5kN	>1.5kN
CTS/TSS	0.28	0.3
Peel	>2kN	>1.5kN
Peel/TSS	0.12	0.3
TSS Fatigue (10^7)	0.75kN	0.75kN

3.6 **Testing**

3.6.1. **Lap-Shear Tension**

Lap-shear tension was the first testing configuration examined. The coupons used measured 100 mm x 25 mm. A coupon of each material was placed in the FBJ fixture, with a 25 mm overlap. The joint configuration for lap-shear tension is shown in Figure 3-10. Fifteen specimens each of external and internal bits were used for comparison. The specimens were welded, alternating the head design every five specimens. The specimens were tested using an Instron machine. The specimens were placed in the machine with aluminum and steel shims in order to maintain the pull direction perpendicular to the weld axis. This is shown in Figure 3-11. The specimens were pulled at a rate of 10.16 mm/min at room temperature. Elongation and max load were collected using the machine software. Designated specimens were sectioned using a Wire EDM. These sections were cut along the short axis through the exact center of the joint. The sections were then placed in Bakelite and sanded using silicon carbide sandpaper. After polishing, the specimens were etched with a 5 percent Nital solution.

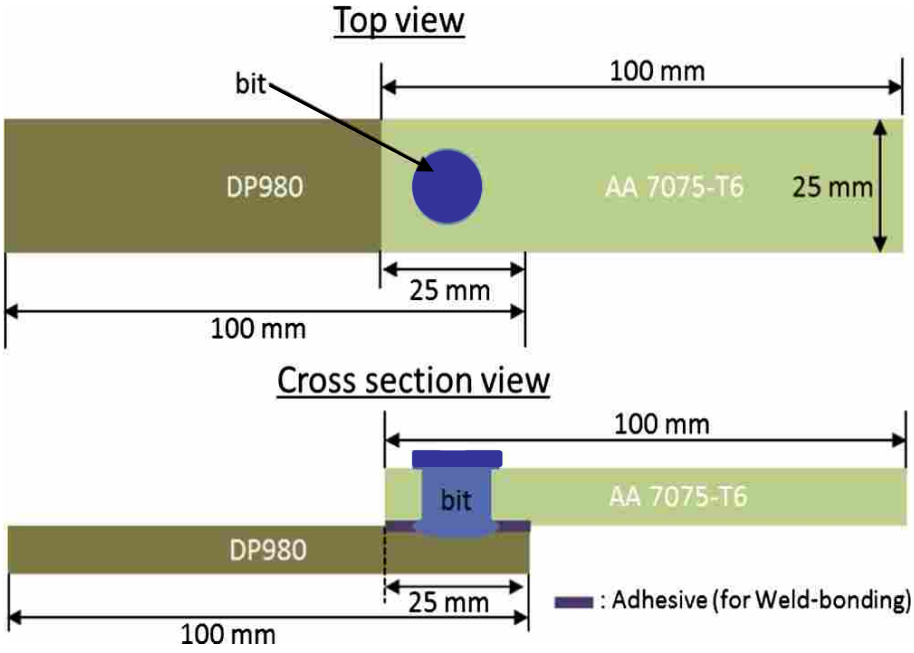

Figure 3-10: Lap-Shear Tension Joint Configuration

Figure 3-11: Lap-Shear Tension Testing in Instron

3.6.2. **Cross-Tension**

The coupons used for cross-tension were wider than those for lap-shear tension testing. The coupons measured 150 mm x 50 mm. They also had two ¾ inch alignment holes on each end. Figure 3-12 depicts the specimen configuration for cross-tension testing. Only external bit welds were cross-tension tested. The weld specimens were placed in the same Instron machine as lap-shear testing, but using a different fixture (Figure 3-13). A tensile load was applied on the weld in a direction normal to the weld.

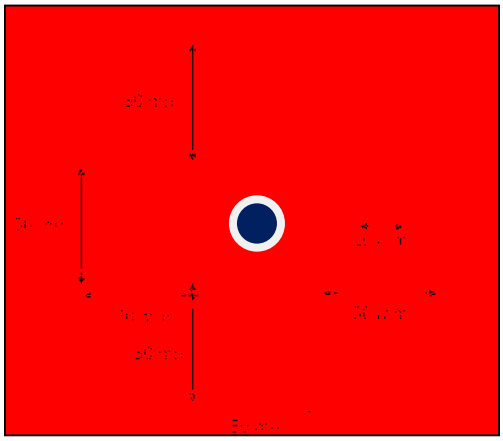

Figure 3-12: Cross-Tension Specimen Configuration

Figure 3-13: Cross-Tension Testing Fixture with Specimen Placed

3.6.3. **Peel**

Peel testing is used for evaluating crash worthiness of joints. Three sets of specimens were made for peel testing joints. The coupons used for all specimens were the same as lap-shear tension testing. For welding, the aluminum was placed directly on top of the steel, with full overlap. Only external bits were used. For the first specimen set, the specimens were manually bent 25 millimeters from the end after the joints were made. The specimens were held in a vise with aluminum shields bent past the desired radius. The initial bending radius was too small, and the aluminum broke off. The radius was increased and manually bent both coupons 90 degrees to form a 180 degree total plane. The vise setup is shown in Figure 3-14. The specimens were then tested on the Instron machine.

Figure 3-14: Vise Setup for Peel Specimen Bending

For the next set of specimens, the material was bent twenty millimeters from the end. This would decrease the moment arm and hopefully increase the tensile strength. During welding, we noticed slight vibration at the tail of the coupons. For the last set of specimens, we

used a C-clamp placed at the tails of the coupons. We also ran lap shear specimens throughout the procedure to use as a control. We bent the specimens at twenty millimeters again.

The final attempt during this research to increase peel strength was to make specimens according to a configuration determined by a standard. An ISO standard was purchased, and the width and length of the coupons were increased to match the standard dimensions. The location of the weld was adjusted to reflect the new coupon dimensions. An attempt was made to decrease the bending radius to the thickness of our thinnest material (1.2 mm), but it was unsuccessful. The aluminum is not ductile enough to bend that severely. The original 7 mm radius was maintained. Bending was performed slowly in order to reduce material failure during bending. The new specimens were tested on the Instron machine with a lap-shear tension specimen for a control. The placement in the Instron machine was also according to the standard. Figure 3-15 shows a peel testing specimen with the new standard dimensions, and Figure 3-16 shows the specimen in the Instron machine.

Figure 3-15: Bent Peel Testing Specimen

Figure 3-16: Peel Testing Specimen in Instron Machine

3.6.4. **Fatigue**

Lap-shear tension specimens were fabricated for fatigue testing. A different Instron machine was used for fatigue testing, because it had more capability than the other Instron machine. The specimens were placed in the machine, again using shims for alignment. The applied load cycled between 100 N and 750 N. The specimens were tested at a frequency of 13 Hz for the first specimen and 20 Hz for the other two specimens. The specimens were tested to failure. The data from each test was outputted to a spreadsheet for analysis.

3.7 **Model Validation**

A finite element model was created to predict aspects of the FBJ process, including: welding temperatures, material flow, bond area, and welding loads. Using the same coupon dimensions as the lap-shear testing coupons, specimens were fabricated to validate this model. Only the steel coupons were used for the model validation experiments, because the cutting stage was not included in the model. The cutting stage was not included in the model, because the effect it had on material flow was not necessary for obtaining adequate weld predictions with the simulation model. It was not included for simplification purposes. A bit with a straight shaft, no cutting flutes, was used, and the bit heads were the externally driven design. After the welds were made, they were sectioned, and specimens were made using the same process as the lap-shear sections. The polished specimens were examined under a microscope and bond area was measured. Load and temperature data was also collected during welding for comparison to the model. Three thermocouples were placed below the weld location in order to measure temperatures. The welds simulated in the model used a bit speed (spindle speed) of 2500 rpm, plunge rate of 200 mm/min, plunge depth of 1.9 mm, and weld time of 0.8 seconds.

4 RESULTS AND ANALYSIS

4.1 Lap-Shear Tension

There are four main failure modes for tension testing of FBJ joints: head, nugget, material, and interfacial. Head failure occurs when the bit head separates from the bit shaft during testing. Nugget failure occurs when the weld nugget tears out, with the bit and coupon material otherwise intact. Material failure is characterized by the bit and weld remaining intact, but the coupons have separated because one of the materials reached its UTS. The fourth failure mode, interfacial failure, is observed when there is separation of the coupon materials at their interface. Also, bit material is observable in both coupon materials. It is also possible to get a combination of interfacial and nugget pullout. In this case, a portion of the nugget is pulled out of one of the sheets and the rest of the nugget shears at the interface (Radakovic, 2012). The four main failure modes can been seen in Figure 4-1 (Squires, 2015). The most common failure modes observed during this research were interfacial.

Figure 4-1: Failure Modes

Nugget pullout failure is the most desired failure mode for joints made through RSW, and interfacial failure is the least desired. This is because joints that fail in nugget pullout are assumed to have better energy absorption (Marya, 2005). However, for FBJ, it is not certain if interfacial failure is a result of an insufficient joint strength. During RSW, greater heat is generated than in FBJ, and therefore, has a larger HAZ. This heat tempers the material in the HAZ and softens the material. This softer region is more susceptible to failure (Marya, 2005). In FBJ welds, the HAZ zone is smaller, and so more of the force is focused on the joint itself. This could be an explanation for the increased amount of interfacial failure. For lap-shear tension testing, the strength was adequate despite experiencing interfacial failure.

The desired performance for lap-shear tension testing according to automotive standards is for the failure load to be greater than 5 kN. The welds created with externally driven bits had a mean peak load before breaking of 12.9 kN, with a standard deviation of 0.8 kN. The welds created with internally driven bits had a mean peak load before breaking of 12.9 kN, with a standard deviation of 0.7 kN. The external welds had higher minimum and maximum loads than the internal bits. The mean for internal bits was slightly higher and had a lower standard deviation. Table 4-1 gives the results from the 30 welds created for lap-shear tension testing.

All 30 specimens experienced interfacial failure. There was one specimen in which the failure occurred higher in the bit shaft, but it would still be characterized as interfacial failure. Sheet thickness has been found to have an effect on failure modes for spot welding. In a study by Marya and Gayden, it was found that 1.8 mm-thick DP600 steel showed lower susceptibility to weld interfacial failure than the 2.0 mm DP600 steel. (Marya, 2005) The research for the current project was the first to use 2 mm thick AA7075, compared to the 1.4-1.6 mm AA used in previous research. This increase in top material thickness may explain the lack of other failure

modes. The aluminum used in previous FBJ was also not as strong as the AA 7075. This increase in material strength might also have influenced the modes of failure for this research.

Table 4-1: Lap-Shear Tension Test Results

External Bits			Internal Bits		
	Extension at Machine Peak Load (mm)	Load at Machine Peak Load (N)		Extension at Machine Peak Load (mm)	Load at Machine Peak Load (N)
1	3.98780	13344.66600	16	3.73380	13464.76799
2	4.08940	13820.62575	17	3.45440	13140.04779
3	3.07340	12539.53782	18	3.27660	12859.80980
4	3.47980	13104.46201	19	3.40360	13100.01379
5	3.58140	12859.80980	20	3.68300	12721.91492
6	3.93700	13384.70000	21	3.07340	10706.87035
7	3.83540	13745.00598	22	3.96240	13384.70000
8	2.74320	11396.34476	23	3.70840	12824.22403
9	3.50520	13046.63513	24	3.83540	12815.32758
10	3.35280	12072.47451	25	3.93700	13722.76487
11	3.12420	12192.57650	26	3.55600	12819.77580
12	3.53060	13478.11266	27	3.93700	13704.97198
13	3.30200	12223.71406	28	3.42900	12984.36002
14	3.37820	11810.02941	29	3.35280	12330.47138
15	3.65760	13696.07554	30	3.42900	13171.18534
Min	2.74320	11396.34476	Min	3.07340	10706.87035
Max	4.08940	13820.62575	Max	3.96240	13722.76487
Range	1.34620	2424.28099	Range	0.88900	3015.89452
Standard Deviation	0.36771	765.67302	Standard Deviation	0.26861	719.11433
Mean	3.50520	12847.65133	Mean	3.58479	12916.74704

The mean peak load for both bits is above the standard 5 kN for the automotive industry. The external bit mean is 2.57 times the standard requirement. Although there is a slightly greater standard deviation, the welds with external bits show comparable joint strength to those with

internal bits. Based on these results, the hypothesis that the external bit will perform comparably to internal bits and meet automotive requirements for joint performance is maintained.

An unpaired t-test was performed to compare the load data of the two bit designs. The results from the test are given in Table 4-2. With a 95 percent confidence interval, it was found that the difference between the means was not statistically different. This means that changing to the external bits did not have a statistical impact on the joint strength, and it can be assumed that the external bit is not worse than the internal bit. Only external bits were evaluated for cross-tension, peel, and fatigue, because of the assumption that the internal and external bits would perform similarly, and future research will be focused on the external design.

Table 4-2: Values Used for Calculating T-Test

P value	0.8008
t value	0.2548
df value	28
std error of difference	271.217
95% confidence interval	From -624.659 to 486.467

Figures 4-2 and 4-3 show the graphs for two specimens comparing extension to the lap-shear tension load. A linear relationship is shown between the lap-shear load and extension. The graphs for both specimens are almost identical. This further demonstrates that external and internal bit specimens perform similarly. Figure 4-4 shows a graph of the maximum tensile load versus maximum extension for all specimens. These graphs show that as extension increases as the lap-shear load increases.

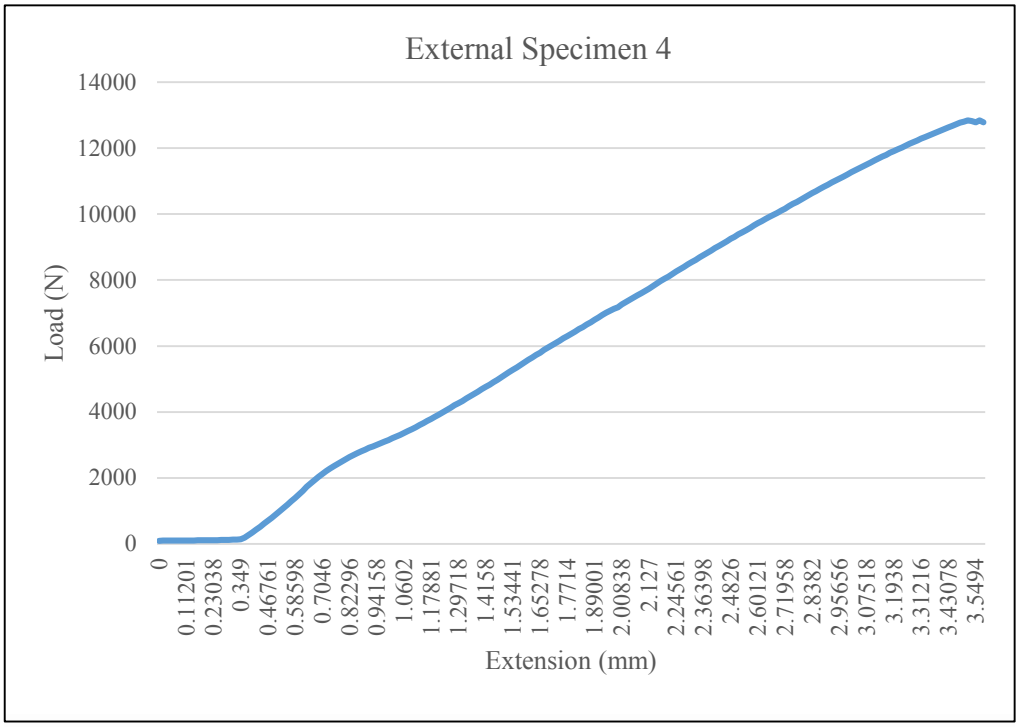

Figure 4-2: Load vs. Extension for External Specimen

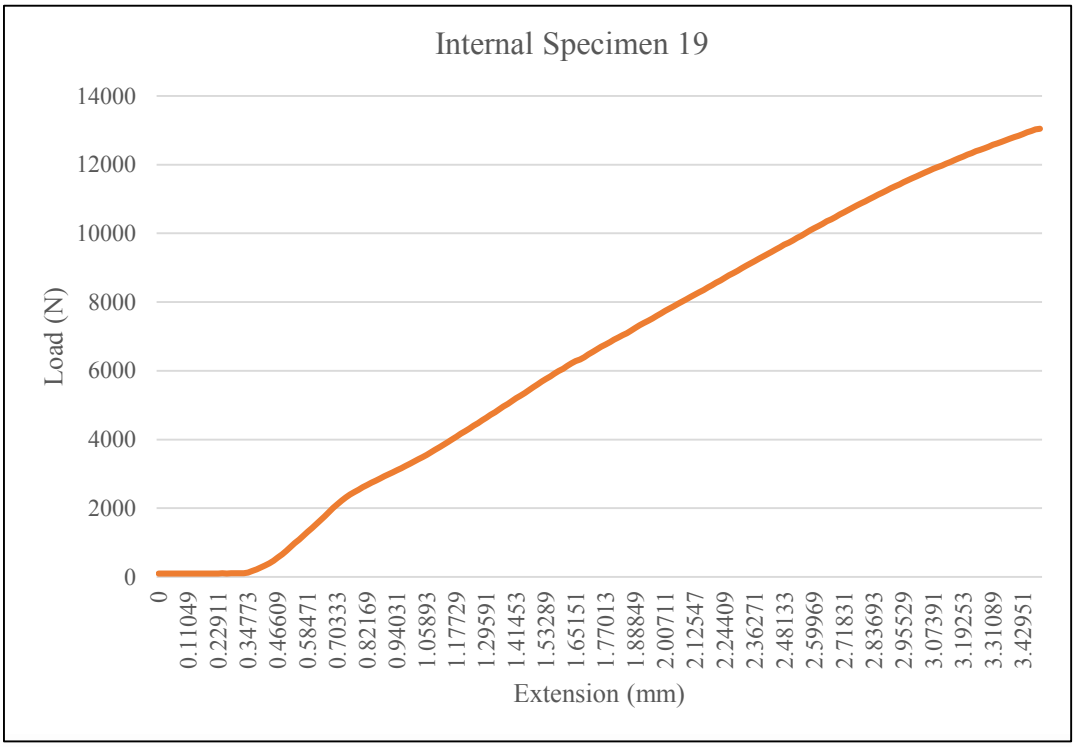

Figure 4-3: Load vs. Extension for Internal Specimen

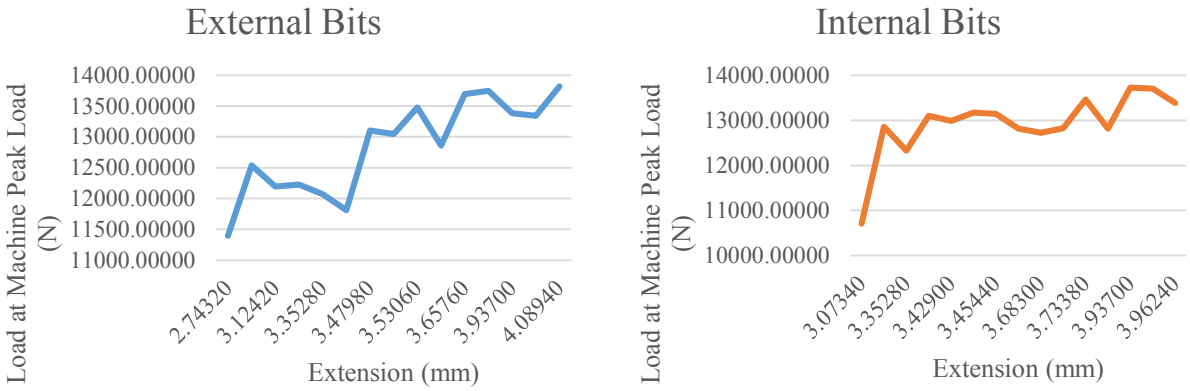

Figure 4-4: Lap-Shear Specimens Load vs. Extension

Three lap-shear tension specimens were cross-sectioned, polished, and set in Bakelite. They were then examined under a microscope and bond length was measured. It was assumed that the welds were symmetrical about the center axis, and a cross-section would provide adequate information about the entire weld. The voids that were observed with the internal bits are eliminated, and the head is solid. Sharp "V's," illustrated in Figure 4-5, are observed where the base material and bit meet. The distance from the points of the "V's" was measured as the bond length. For spot welding, weld size has a significant effect on failure mode and weld strength (Hernandez, 2008). Weld size, or nugget diameter, is typically slightly less than the diameter of the impression the electrode creates on the material. Weld size can be compared to bond area in processes such as FSSW and FBJ. For FSSW, bond strength can be correlated to the bonded area created during the spot welding process (Saunders, 2014). Therefore, by increasing the bond area of FBJ welds, joint strength can increase and nugget failure will more likely be achieved. A suggestion for increasing bond area would be to increase the hardness of the bit material. This would cause the bit to plunge deeper into the base material with less shearing.

With the current bit material, 4140, as plunge depth increases, the bit begins to shear more, compromising the integrity of the joint strength.

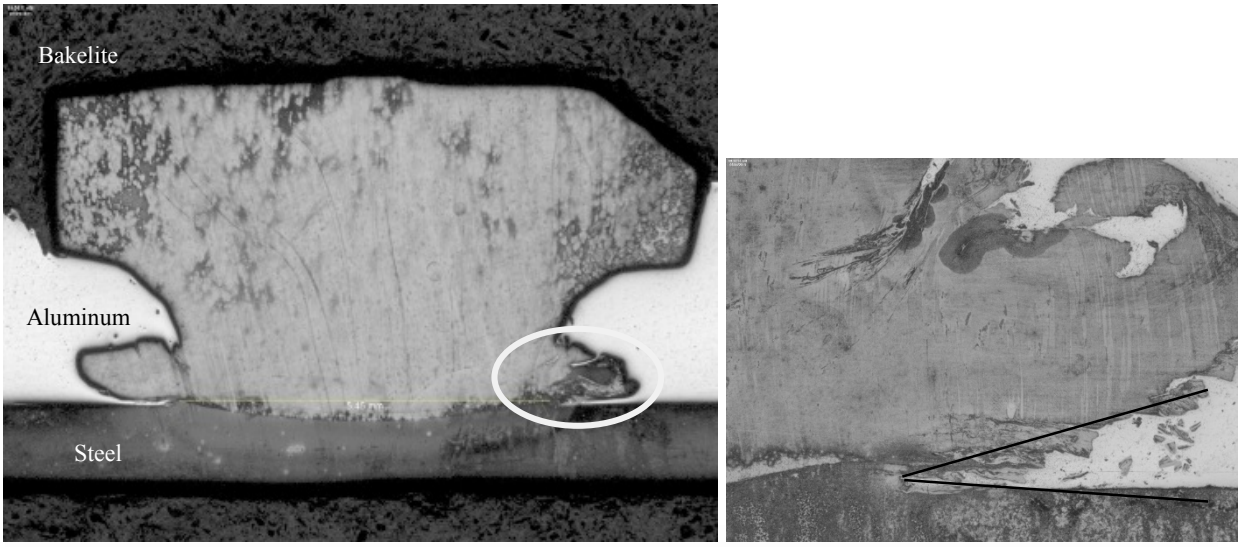

Figure 4-5: Lap-Shear Specimen Cross Section and Detail View of Right Side

4.2 **Cross-Tension**

Cross-tension is a more severe test to the joints than lap-shear tension. All of the six specimens experienced interfacial failure. For two of the specimens, fracture of the joint led to a large amount of the bit shaft remaining on the base material. This is shown in Figure 4-7. One explanation for these results is cross-tension forces being placed directly upon the interface between the bit head and shaft.

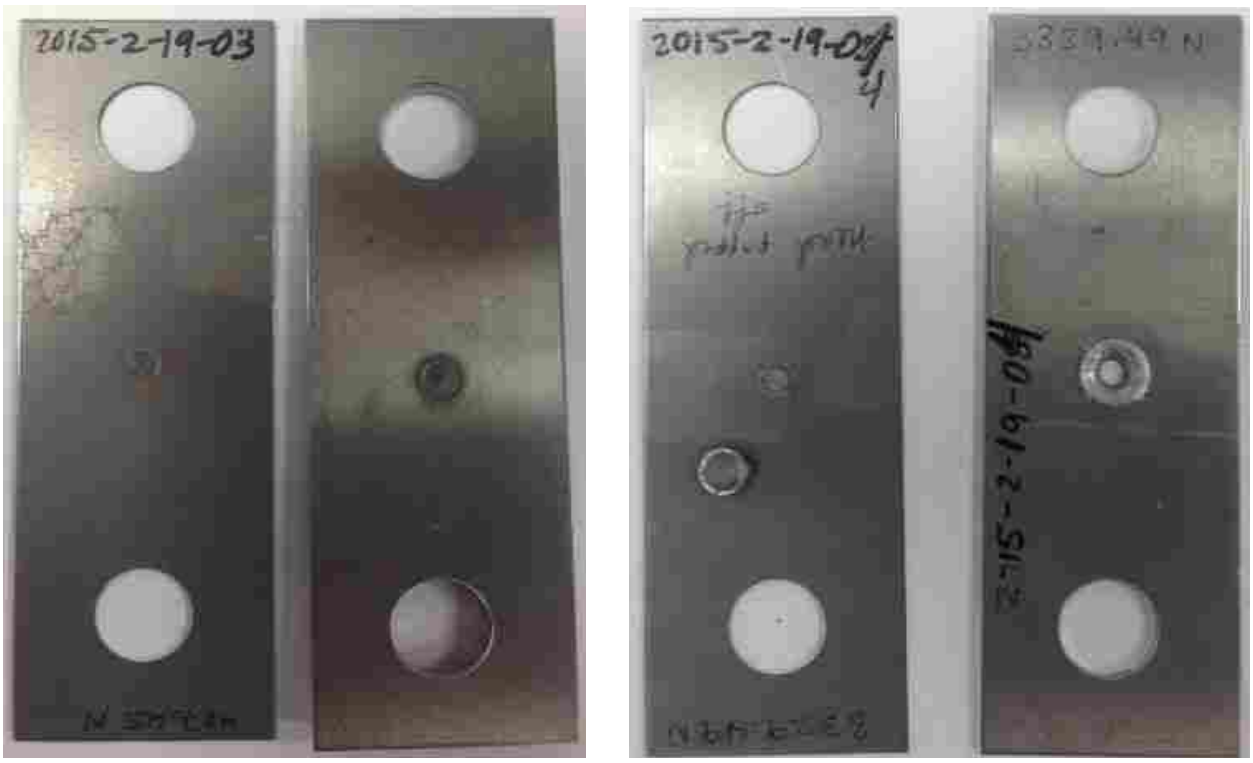

Figure 4-6: Cross-Tension Interfacial Failure Modes

In previous testing at BYU, cross-tension specimens were made with the same weld parameters, FBJ machine, and internal bit design as those used in the current study. The average tensile strength for five cross-tension experiments was found to be 2.88 kN (Squires, 2014). These results are comparable to the results found with the research conducted for this project.

The results from the cross-tension testing are given in Table 4-3. For the six cross-tension tests, the average tensile strength was found to be 2.818 kN, with a standard deviation of 0.340 kN. The average joint strength for cross-tension testing was 1.88 times more than the standard required by Honda. The minimum peak load was 2.427 kN, which is still almost a kilonewton above the standard. This shows that joints made with external bits exceed the required performance and create a strong enough joint. Based on these results, the hypothesis that the

external bit will perform comparably to internal bits and meet automotive requirements for joint performance is still maintained.

Table 4-3: Cross-Tension Test Results

	Extension at Machine Peak Load (mm)	Load at Machine Peak Load (N)	Failure Mode
1	4.08940	2426.50510	Interfacial
2	5.08000	2731.20831	Interfacial
3	4.29260	2487.44574	Interfacial
4	5.38480	3329.49417	Head/Interfacial
5	5.46100	2928.26454	Head/Interfacial
6	5.68960	3004.32914	Interfacial
Maximum	5.68960	3329.49417	
Minimum	4.08940	2426.50510	
Standard Deviation	0.65911	340.16766	
Mean	4.99957	2817.87450	

4.3 **Peel**

Peel testing is the most severe of the tests performed during this research. It is also very important for demonstrating crash worthiness for automotive applications. Three different sets of experiments were performed for peel testing. All of the specimens experienced interfacial failure, shown in Figure 4-8.

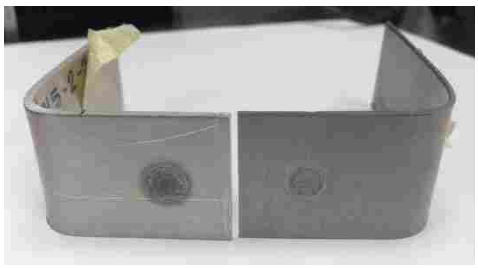

Figure 4-7: Peel Testing Interfacial Failure

As peel testing began, it was found that the load at failure was significantly lower than the standard. Modifications to setup and bending were made in order to eliminate possible causes. After the first five specimens from the third set were tested, no significant improvement was noticed. The lap-shear specimen that was tested yielded a reasonable peak load. The automotive standard for peel failure is 1.5 kN. The results from these three tests, given in Table 4-4, do not achieve the required joint strength for the automotive standard. Peel testing of internal bits has not been conducted, and a comparison is not available.

Table 4-4: Peel Testing Results for Three Iterations of Testing

Iteration 1			Iteration 2			Iteration 3	
	Load at Machine Peak Load (N)			Load at Machine Peak Load (N)			Load at Machine Peak Load (N)
1	349.85		1	567.15		1	225.66
2	329.57		2	377.20		2	364.18
3	370.18		3	538.68		3	353.46
4	363.02					4	280.59
5	435.84					5	458.61
6	540.90						
Maximum	540.90		Maximum	567.15		Maximum	458.61
Minimum	329.57		Minimum	377.20		Minimum	225.66
Standard Deviation	78.55		Standard Deviation	102.44		Standard Deviation	88.57
Mean	398.23		Mean	494.34		Mean	336.50
						Lap-shear Control	12615.16

An idea for improving the joint strength was to bend the specimens according to a standard. An ISO standard was acquired, and the dimensions were compared to that of the standard. The length and width of the coupons were about 20 mm larger in the standard than what was being used. Adjustments to coupon size and location of weld were modified to reflect

the standard. The bending radius was also decreased. A lap-shear sample was again used as a control. Table 4-5 shows the results from the final peel testing. Although the procedure for testing was adjusted to reflect a standard setup and procedure, with the exception of bending radius, the maximum load that the samples broke at did not change. The results reflected the results in previous testing.

Table 4-5: Results from Peel Tests Bent According to Standard

Specimen	Load at Machine Peak Load (N)
1	322.407
2	392.867
3	265.070
4	472.846
5	298.520
Maximum	472.846
Minimum	265.070
Standard Deviation	82.995
Mean	350.342

In bending, the outer structure of the material is in tension while the inner structure is in compression. As the bending radius decreases, the tensile load on the outer fibers increases. This can eventually lead to failure of the material. This was experienced during the bending of the material for the experiments in this research. A larger bending radius was necessary in order to keep the specimens intact and perform testing. Typical bending practices use a bending radius of two to three times the thickness of the material being bent. This would result in a bending radius of at least 6 mm for the aluminum in this experiment. The standard used for the bending configuration called for a bending radius equal to the thickness of the thinnest material used. This would be 1.2 mm, being dictated by the DP980. AA 7075, because of its high-strength

properties, has lower ductility. Table 3-3 shows that AA 7075 has a percent elongation of only 5-8. This is half of the 12.5 percent demonstrated by the DP980. This low-percent elongation explains the difficulty in bending the aluminum to a lower radius. A more controlled bending process may allow the material to be bent further, but the resources for this research were not sufficient for a smaller bending radius. A larger bending radius increases the moment arm, and therefore increased the force being applied to the joint. Decreasing the bending radius and subsequent moment arm will improve the performance of joints tested in the peel configuration.

While examining sectioned specimens under the microscope, an area of concern was observed. This was micro-cracks in the bit and weld. Figure 4-6 shows views of the sectioned weld with emphasis on the micro-cracks. These defects might be the cause of the variability experienced in joint performance, the low maximum peel failure load, and the interfacial failure. In a study by Bisadi, et al, they found that increasing the formation of micro-cracks led to a reduction in the ultimate tensile strength in tensile shear testing of friction stir spot welded joints (Bisadi, 2013). Interfacial failure of spot welds is a result of crack propagation through the weld nugget (Chao, 2003). In the case of the FBJ welds of this research, the micro-cracks found near the weld interface would be susceptible to propagation and may have been a cause of the interfacial failure.

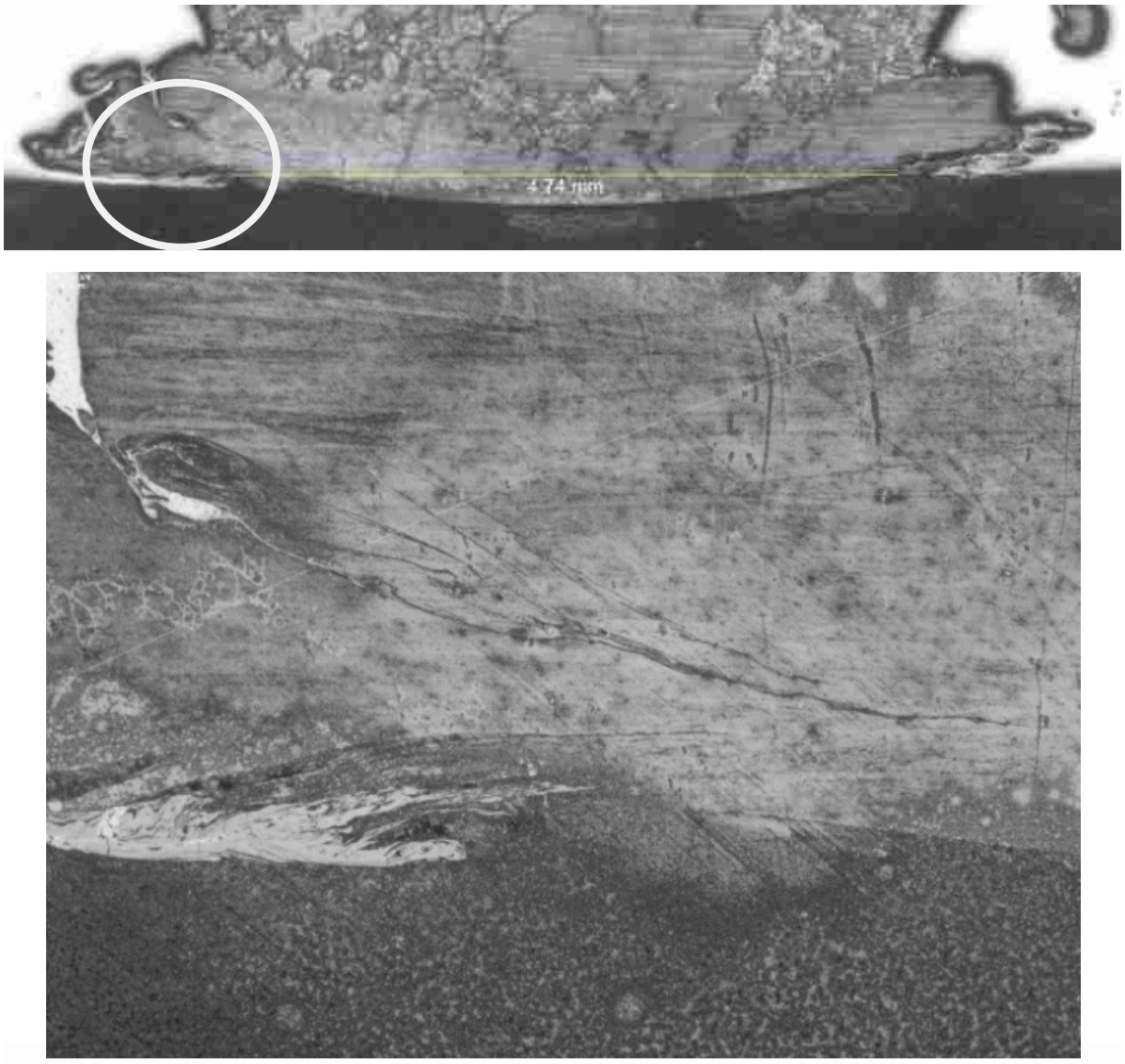

Figure 4-8: Micro-Cracks in Sectioned Weld

The micro-cracks may be caused by the shearing of the bit during welding. As the rotating bit makes contact with the DP980, the bit shears, and as it solidifies, the micro-cracks form. The increased spindle speed during the second stage of the process has shown to reduce bit shearing and increase joint strength (Squires, 2014). Shearing can also be reduced by increasing the hardness of the bit. In the current research, the 4140 steel and the DP980 steel have about the same hardness. Increasing the hardness of the bit would raise its ability to penetrate the steel

before shearing. This would increase the bond area as well as reduce the presence of micro-cracks. Joint strength would then be increased.

4.4 **Fatigue**

Fatigue testing is important for automotive applications. In this research, three specimens were tested for fatigue. The specimens demonstrated failure by either interfacial failure of the joint or plastic deformation of the specimen. The latter case was exhibited when the machine was not able to reach the set load values in the given cycle time established by the frequency or increased extension over time. The number of cycles to failure varied for the specimen set. This variability could be explained by the micro-cracks along the weld zone. The standard set by Honda for desired performance in service is to reach at least 10 million cycles before failing, under a cyclic load of 0.1-0.75 kN. All three specimens surpassed 10 million cycles before failure. These high numbers for cycles to failure may be attributed to the relatively low load of 750 N that is used for testing.

Table 4-6: Fatigue Testing Cycles to Failure

Specimen No.	Frequency (Hz)	Cycles to Failure (10^7)
1	13	16.627
2	20	25.267
3	20	20

Specimen 2 demonstrated failure through plastic deformation. Figure 4-9 shows a graph of extension over time for Specimen 2. The extension began to increase and then taper off and become a more narrow range. This demonstrated that the specimen had failed. Specimen 1 experienced interfacial failure. For fatigue testing lap-shear spot welds, cracks normally initiate

at the edge of the nugget button or in the HAZ. The cracks then propagate through the joint causing interfacial failure. “These defects result in a stress concentration and an increase in the triaxiality of the local stress state to facilitate the crack initiation and accelerate the crack growth rate” (Ma, 2007). In the FBJ samples of this research, micro-cracks near the bond interface contain high-stress concentration due to welding (Figure 4-6). As the joints are tested, the cracks propagate through the weld causing interfacial failure (Rathbun, 2003). The length and number of micro-cracks varied between specimens. This variance may be the cause of the large standard deviation for cycles to failure in fatigue testing and the maximum load for mechanical testing. Fatigue life may be extended by strengthening the microstructure of the welds, because the fatigue life is dependent upon the time the cracks in the joint spend propagating through the weld (Rathbun, 2003).

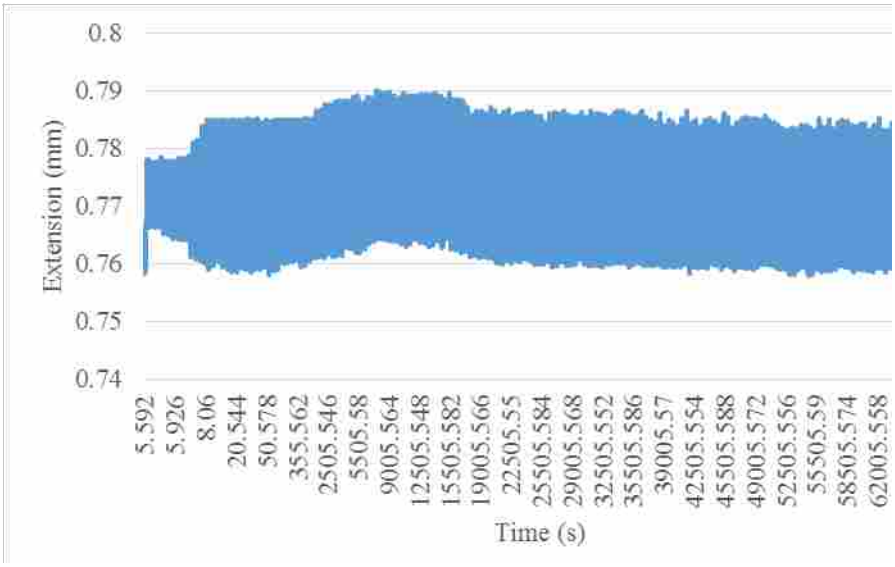

Figure 4-9: Extension vs. Time for Specimen 2

4.5 **FBJ Process Model**

The Forge® finite element software was used to create the model simulation. A simulation model of the process was used to predict temperatures in the weld zone as well as the final bond area created by welding, for a given bit design and for a given set of alloys.

A model of the FSSW process was developed using a finite element approach within the Forge® software package. An updated Lagrangian scheme with explicit time integration was employed to model the flow of the sheet material, subjected to boundary conditions of a rotating tool and a fixed backing plate. The modeling approach is two-dimensional, axisymmetric, but with an aspect of three dimensions for thermal boundary conditions. Material flow was calculated from a two dimensional velocity field, but heat generated by friction was computed using the virtual sliding velocity between the sheet and the tool. These heat terms where then used as boundary conditions for the coupled thermal calculation between tool and sheet. An isotropic, viscoplastic Norton-Hoff law was used to model the evolution of material flow stress as a function of strain, strain rate, and temperature. One half of a section view of the model is shown in Figure 4-10, with a simplified bit design for validation purposes. The bit material is alloy 4140 (green), the sheet is DP 980 (red), and the backing plate (yellow) is plain carbon steel. The locations where temperature was measured experimentally are shown with dots in the backing plate. Validation of the model was done experimentally by measuring welding temperatures at three different locations below the sheet, in the backing plate.

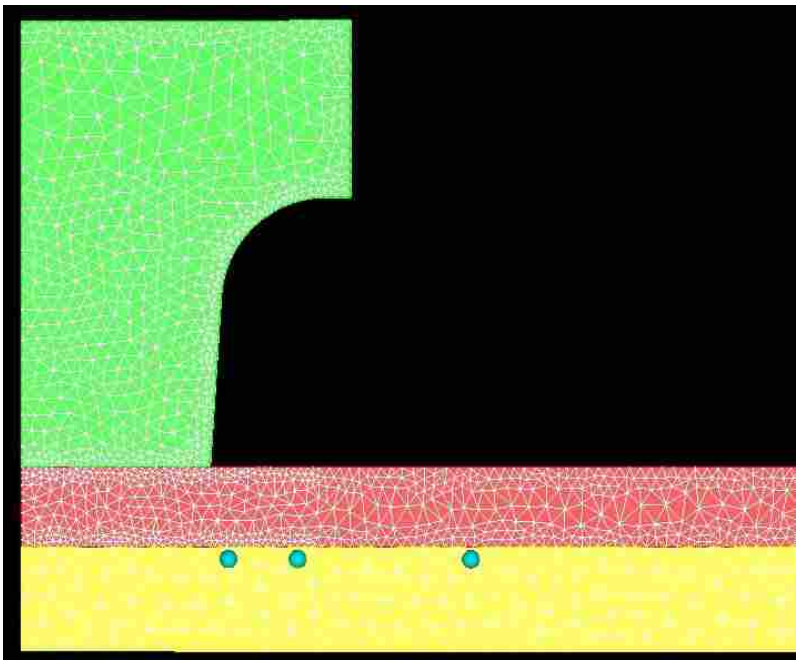

Figure 4-10: Friction Bit Joining Model, with Simplified Bit Design and No Aluminum Top Sheet.

The specimens created for model validation were examined under a microscope after welding. Bond length was then measured and compared to the model result. Figure 4-11 shows one of the sectioned welds. The average bond length of the specimens was 6.29 mm, with a standard deviation of 0.547 mm. The bond length predicted by the simulation was 6.57 mm, so the bond length prediction was accurate to within 5 percent.

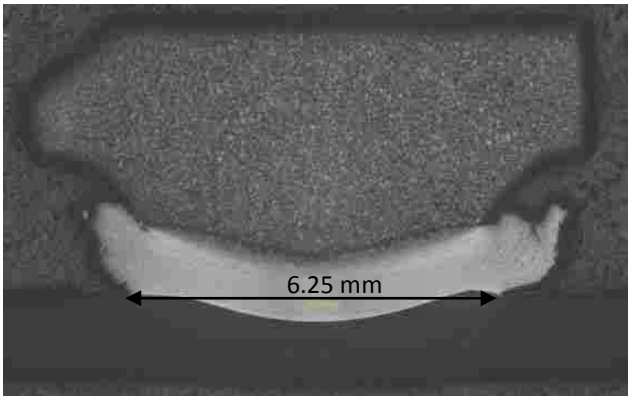

Figure 4-11: Cross-Section View of Bit to Steel Weld for Model Validation

The predicted weld shape was also compared between the experiments and the simulation. The simulation was able to predict a similar, though more simplified, shape for the welds created with FBJ. Figure 4-12 shows the simulated weld shape compared to the experiment.

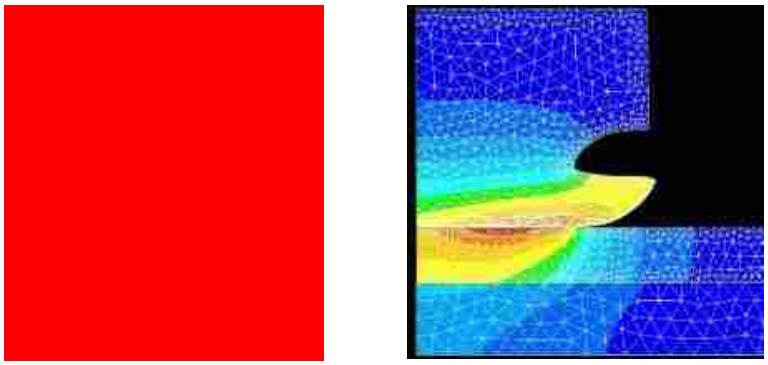

Figure 4-12: Experiment v.s Simulation Weld Shape

The three different locations of the thermocouples for the experiments were replicated for the simulation, as seen previously in Figure 4-10. The peak welding temperatures were tracked for all three locations. Table 4-7 shows the peak temperatures for the experiment compared to the simulation. The temperatures closer to the weld location have a greater difference between the experiment and simulation. Further work is needed on both the experimental and modeling sides of the project. During welding, the thermocouples would shift easily. Temperature measurements can be improved by fine-tuning the experiment setup process and adjusting the method for placement and holding of the thermocouples. This would improve temperature readings for comparison to the simulation model. For modeling, the heat transfer coefficient can be altered to improve temperature predictions.

Table 4-7: Peak Temperatures for Model Validation Experiment and Simulation

Comparison	Experiment	Simulation	Difference
Temperature at 3mm	245 °C	294 °C	49 °C
Temperature at 4mm	152 °C	217 °C	65 °C
Temperature at 6.5mm	94 °C	79 °C	15 °C

4.6 **Other Benefits of Externally Driven Bits**

The external bits were also evaluated according to manufacturability. The internal bits are made using only cutting processes on a CNC lathe. From start the finish, it takes on average 2.78 minutes to complete one bit. The cutting processes used to make these bits are more expensive than a forming process would be. This is one reason changing to the external bit design is an improvement. It takes an average of 2.20 minutes to finish one external bit. This time could be reduced significantly by using an additional forming die. While one bit blank is being pressed in one die, another bit blank can be prepped in the other die. The changeover would then be changed to an external process. Although the initial step of cutting blanks on the CNC lathe is the same, the cold forming process is less expensive. In addition to cycle time being less for external bits, the manufacturing process is similar to other small part manufacturing processes, for example: bolts. The manufacturing process would then be an adaptation of an existing process. Whereas, the internal bits would need an entirely new system to manufacture. The external bits will cost less to manufacture than the internal bits because of cycle time, equipment, and process cost savings. This cost savings makes the external bit a better candidate for implementation in high-volume applications.

Corrosion is another area of concern for joints and application, especially with dissimilar metal combinations. Joints made with FBJ must be able to maintain strength while in service. Galvanic corrosion is a common form of corrosion experienced with lap-joints of AA 7075 and DP980 with an ANSI 4140 bit. This occurs when two dissimilar metals are in electrical contact in an electrolyte (Lim, 2015). The addition of an adhesive layer can alleviate problems caused by galvanic corrosion. The type of corrosion that is lessened by implementation of the external bits is crevice corrosion. This occurs when small volumes of stagnant solution are localized in confined places (Lim, 2015). This was a problem that could be experienced with the internal bits because of the internal cavity necessary for driving the bits. The external bits eliminate this internal cavity, and can minimize the corrosion medium infiltration path.

The automotive industry is a high-volume, high-speed, and highly controlled manufacturing environment. FBJ and its components must be suitable for this application. Therefore, bits were evaluated according to ease of automation. The design of the external bits and driver allow the driver to rotate until the bit is engaged properly. Then the bit is driven. The internal bits, however, must be placed in the correct orientation onto the driver in order for them to be engaged properly. The alignment simplicity of the external bits is ideal for automation applications. The external bits are more optimally designed for automation than the internal bits.

4.7 **External Bit Manufacturing Process Improvements**

There are several process improvements that can be employed to reduce variability and increase efficiency. The first is to use multiple forming dies while making bits. This will allow the changeover to be performed while another bit is being formed, and about 15 seconds can be saved per bit. Another tool that will improve the bit-making process is a right-handed insert for

the parting tool. A right-handed insert would help with the pip that remains after machining the bit blanks. With a right-handed insert, the leading corner of the cutting edge is next to the part being cut off. The pip is then left on the workpiece while still in the machine. This new insert would hopefully eliminate the step of grinding off the excess material before forming the blanks. The feed rate during turning would need to be altered in order to reduce the size or severity of the pip left on the bit blanks.

Significant variability is introduced when placing the external bits into the driver. The magnet used has enough strength to hold the bits in the driver. However, the bit does not easily set into the driver, because the diameters of the driver and the bits do not have enough difference. To compensate for this, bits were forced into place with a rubber mallet to ensure correct placement in the drivers. This created significant variability in placement of the bits in the driver. Decreasing the diameter of the bit head would alleviate this problem. When the heads are formed and then placed in the driver, it would be the magnet holding the bits in place rather than force. Decreasing the diameter of the bit head, rather than the diameter of the driver, would reduce the amount of material used for bits and, therefore, save on costs. Joint-strength integrity would need to be examined to ensure the change in bit diameter did not have a negative effect on joint performance.

5 CONCLUSIONS AND RECOMMENDATIONS

5.1 Conclusions

Friction bit joining has proven to join advanced high-strength steels and aluminum. This innovative joining technique can facilitate multi-material structures, resulting in lighter-weight vehicles and better fuel efficiency. FBJ has already been proven as a feasible option for creating joints strong enough for the automotive industry. This research evaluated the improvements of an externally driven bit head design and compared the design to the previous externally driven bit head design. The external bit design was also studied for improvement for manufacturing costs and the ability to be implemented in an automated setting.

Through mechanical testing of lap-shear tension, cross-tension, and peel, the joint strength of welds created with the external bit was evaluated. The external design performed comparably to the internal bit design for lap-shear tension and cross-tension. Joint strength was not sacrificed for those failure modes. Peel test results were not adequate for the standards set by Honda for implementation in service. Further investigation and improvements are necessary to confirm that joints made with external bits are satisfactory for the automotive industry. Fatigue testing of lap-shear tension specimens was also performed and all tested specimens exceed the required 10 million cycles before failure.

The external bit design was also assessed according to manufacturability and ease of automating. The process used to manufacture the external bit heads are less expensive and have a

shorter cycle time. The external bits are less expensive to manufacture than the internal bits. The design of the external bits is also more easily aligned with its driver than the internal bit design with its driver. This ease of alignment makes the external bits more conducive to being applied in an automated setting. The results found in this research do not reject the hypothesis that welds created with externally driven bits will meet the automotive standard service requirements for three of the four criteria. Further research is necessary to assess the peel strength of FBJ welds with external bits.

The bond area predicted by the Forge simulation model was accurate to within 5 percent, and the predicted bond shape was similar to the bond shape created through experiments. Temperature predictions require further study to reduce the difference between the predicted temperatures to the experiment procedures. Once accurate, this model will be valuable for predicting bond area and other parameters for FBJ welds.

5.2 **Recommendations**

Peel testing is the area that the external bit joints performed the poorest. Further examination of bending configuration and welding parameters needs to be explored in order to determine the reason for the poor performance. Decreasing the presence of micro-cracks may increase the joint strength for peel specimens. Micro-crack formation can be reduced by increasing the hardness of the bit. Increasing bond area may also result in an increased joint performance for peel. Reducing micro-crack content and increasing the bond area might also improve joint performance in other testing areas, especially fatigue. The manufacturing process for bits can also be improved. Using the appropriate type and number of tools will reduce cycle time and increase efficiency. Altering the diameter of bits will also improve consistency in joint

performance and reduce material usage. Further study is also needed for complete simulation model building and validation. Reducing errors during experiments will improve temperature measurements, and using various heat transfer coefficients will improve temperature predictions given by the model.

REFERENCES

Abe, Y., T. Kato, and K. Mori. "Self-Piercing Riveting of High Tensile Strength Steel and Aluminium Alloy Sheets Using Conventional Rivet and Die." *Journal of Materials Processing Technology* 209.8 (2009): 3914-3922.

Albrecht, S., M. Baumann, C. P. Brandstetter, R. Horn, H. Krieg, M. Fischer, and R Ilg. "Environmental Aspects of Lightweight Construction in Mobility and Manufacturing." *Green Design, Materials and Manufacturing Processes* (2013): 185.

ALCOA. Alloy 7075 Plate and Sheet. Alcoa Mill Products. (n. d.). Retrieved on 15/5/2015: https://www.alcoa.com/mill_products/catalog/pdf/alloy7075techsheet.pdf

Barnes, T. A., and I. R. Pashby. "Joining Techniques for Aluminium Spaceframes used in Automobiles: Part II—Adhesive Bonding and Mechanical Fasteners." Journal of Materials Processing Technology 99.1 (2000): 72-79.

Billur, M. S., and T. Altan. "Challenges in Forming Advanced High Strength Steels." *Proceedings of New Developments in Sheet Metal Forming* (2012): 285-304.

Bisadi, H., A. Tavakoli, M. T. Sangsaraki, and K. T. Sangsaraki. "The Influences of Rotational and Welding Speeds on Microstructures and Mechanical Properties of Friction Stir Welded Al5083 and Commercially Pure Copper Sheets Lap Joints." *Materials & Design* 43 (2013): 80-88.

Caffrey, C., K. Bolon, H. Harris, G. Kolwich, R. Johnston, and T Shaw. *Cost-Effectiveness of a Lightweight Design for 2017-2020: An Assessment of a Midsize Crossover Utility Vehicle*. No. 2013-01-0656. SAE Technical Paper, 2013.

Chao, Y. J. "Failure Mode of Spot Welds: Interfacial versus Pullout." *Science and Technology of Welding and Joining* 8.2 (2003): 133-137.

Feng, Z., M. L. Santella, S. A. David, R. J. Steel, S. M. Packer, T. Pan, M. Kuo, and R. S. Bhatnagar. "Friction Stir Spot Welding of Advanced High-strength Steels-A Feasibility Study." No. 2005-01-1248. SAE Technical Paper, 2005.

Hernandez, B. V. H., M. L. Kuntz, M. I. Khan, and Y. Zhou. "Influence of Microstructure and Weld Size on the Mechanical Behaviour of Dissimilar AHSS Resistance Spot Welds." *Science and Technology of Welding and Joining* 13.8 (2008): 769-76. Web.

Huang, T., Y.s. Sato, H. Kokawa, M.p. Miles, K. Kohkonen, B. Siemssen, R.j. Steel, and S. Packer. "Microstructural Evolution of DP980 Steel during Friction Bit Joining." *Metall and Mat Trans a Metallurgical and Materials Transactions A* 40.12 (2009): 2994-3000.

Kuziak, R., R. Kawalla, and S. Waengler. "Advanced High Strength Steels for Automotive ndustry." *Archives of Civil and Mechanical Engineering* 8.2 (2008): 103-117.

Lim, Y. C., L. Squires, T. Y. Pan, M. Miles, G. L. Song, Y. Wang, and Z. Feng. "Study of Mechanical Joint Strength of Aluminum Alloy 7075-T6 and Dual Phase Steel 980 Welded by Friction Bit Joining and Weld-bonding under Corrosion Medium." *Materials & Design* 69 (2015): 37-43.

Ma, C., D. L. Chen, S. D. Bhole, G. Boudreau, A. Lee, and E. Biro. "Microstructure and fracture characteristics of spot-welded DP600 steel." *Materials Science and Engineering: A* 485.1 (2008): 334-346.

Marya, M., and X. Q. Gayden. "Development of Requirements for Resistance Spot Welding Dual-Phase (DP600) Steels Part 1—The Causes of Interfacial Fracture." *Welding Journal* 84.11 (2005): 172-182.

Matlock, D. K., and J. G. Speer. "Third Generation of AHSS: Microstructure Design Concepts." *Microstructure and Texture in Steels*. Springer London, 2009. 185-205.

Meschut, G., V. Janzen, and T. Olfermann. "Innovative and Highly Productive Joining Technologies for Multi-Material Lightweight Car Body Structures." *Journal of Materials Engineering and Performance* 23.5 (2014): 1515-1523.

Miles, M. P., Z. Feng, K. Kohkonen, B. Weickum, R. Steel, L. Lev. "Spot Joining of AA 5754 and High Strength Steel Sheets by Consumable Bit." *Science and Technology of Welding & Joining* 15.4 (2010): 325-330.

Miles, M., S. T. Hong, C. Woodward, Y. H. Jeong. "Spot Welding of Aluminum and Cast Iron by Friction Bit Joining." *International Journal of Precision Engineering and Manufacturing* 14.6 (2013): 1003-1006.

Miles, M., U. Karki, and Y. Hovanski. "Temperature and Material Flow Prediction in Friction-Stir Spot Welding of Advanced High-Strength Steel." *JOM*66.10 (2014): 2130-2136.

Mishra, R. S., P. S. De, and N. Kumar. "Dissimilar Metal Friction Stir Welding." *Friction Stir Welding and Processing*. Springer International Publishing, 2014. 237-258.

Mori, K., Y. Abe, and T. Kato. “Self-pierce Riveting of Multiple Steel and Aluminum Alloy Sheets.” *Journal of Materials Processing Technology* 214.10 (2014): 2002-2008.

Pan, T., A. Joaquin, D. E. Wilkosz, L. Reatherford, J. M. Nicholson, Z. Feng, and M. L. Santella. “Spot Friction Welding for Sheet Aluminum Joining.” *Proceedings of the 5th International Symposium of Friction Stir Welding, Metz, France*. 2004.

Pouranvari, M., and S. P. H. Marashi. “Critical Review of Automotive Steels Spot Welding: Process, Structure and Properties.” *Science and Technology of Welding and Joining* 18.5 (2013): 361-403.

Radakovic, D. J., and M. Tumuluru. “An Evaluation of the Cross-Tension Test of Resistance Spot Welds in High-Strength Dual-Phase Steels.” *Welding Journal* 91.1 (2012): 8-15.

Rathbun, R. W., D. K. Matlock, and J. G. Speer. "Fatigue behavior of spot welded high-strength sheet steels." *Welding Journal* 82.8 (2003): 207-218.

Rhodes, C. G., M. W. Mahoney, W. H. Bingel, R. A. Spurling, and C. C. Bampton. “Effects of Friction Stir Welding On Microstructure of 7075 Aluminum.” *Scripta Materialia* 36.1 (1997): 69-75.

Saunders, N., M. Miles, T. Hartman, Y. Hovanski, S. T. Hong, and R. Steel. "Joint Strength in High Speed Friction Stir Spot Welded DP 980 Steel." International Journal of Precision Engineering and Manufacturing Int. J. Precis. Eng. Manuf. 15.5 (2014): 841-48.

Squires, L. P. “Friction Bit Joining of Dissimilar Combinations of Advanced High-Strength Steel and Aluminum Alloys.” (2014). All Theses and Dissertations. Paper 4104.

Sun, X., E. V. Stephens, M. A. Khaleel, H. Shao, and M. Kimchi. "Resistance Spot Welding of Aluminum Alloy to Steel with Transition Material-From Process to Performance-Part I: Experimental Study." *WELDING JOURNAL-NEW YORK*- 83 (2004): 188-S.

Taylor, M.d., K.s. Choi, X. Sun, D.k. Matlock, C.e. Packard, L. Xu, and F. Barlat. "Correlations between Nanoindentation Hardness and Macroscopic Mechanical Properties in DP980 Steels." *Materials Science and Engineering: A* 597 (2014): 431-39.

The Federal Register, EPA and DOT. 2017 and Later Model Year Light Duty Vehicle Green House Gas Emissions and Corporate Average Fuel Economy Standards. Monday, Oct 15, 2012. Washington, DC: EPA and NHTSA; 2012.

Wei, S. T., D. Lv, R. D. Liu, L. Lin, R. J. Xu, J. Y. Guo, and K. Q. Wang. "Similar and Dissimilar Resistance Spot Welding of Advanced High Strength Steels: Welding and Heat Treatment Procedures, Structure and Mechanical Properties." *Science and Technology of Welding and Joining* 19.5 (2014): 427-435.

Weickum, B., "Friction Bit Joining of 5754 Aluminum to DP980 Ultra-High Strength Steel: A Feasibility Study." (2011). All Theses and Dissertations. Paper 2789.